

# Charge storage in nanocrystal systems: Role of defects?

E.W.H. Kan<sup>1</sup>, W.K. Choi<sup>1,2</sup>, W.K. Chim<sup>1,2</sup>, D.A. Antoniadis<sup>1,3</sup> and E.A. Fitzgerald<sup>1,3</sup>

<sup>1</sup>Singapore-MIT Alliance, 4 Engineering Drive 3, Singapore 117576

<sup>2</sup>Department of Electrical & Computer Engineering, National University of Singapore, 4 Engineering Drive 3, Singapore 117576

<sup>3</sup>Massachusetts Institute of Technology, 77 Massachusetts Avenue, Cambridge, MA 02139-66307

**Abstract**—Wet thermal oxidations of polycrystalline  $\text{Si}_{0.54}\text{Ge}_{0.46}$  films at 600°C for 30 and 50 min were carried out. A stable mixed oxide was obtained for films that were oxidized for 50 min. For film oxidized for 30 min, however, a mixed oxide with Ge nanocrystallites embedded in the oxide matrix was obtained. A trilayer gate stack structure that consisted of tunnel oxide/oxidized polycrystalline  $\text{Si}_{0.54}\text{Ge}_{0.46}$ /rf sputtered  $\text{SiO}_2$  layers was fabricated. We found that with a 30 min oxidized middle layer, annealing the structure in  $\text{N}_2$  ambient results in the formation of germanium nanocrystals and the annealed structure exhibits memory effect. For a trilayer structure with middle layer oxidized for 50 min, annealing in  $\text{N}_2$  showed no nanocrystal formation and also no memory effect. Annealing the structures with 30 or 50 min oxidized middle layer in forming gas ambient resulted in nanocrystals embedded in the oxide matrix but no memory effect. This suggests that the charge storage mechanism for the trilayer structure is closely related to the interfacial traps of the nanocrystals.

**Index Terms**—charge storage, defects, germanium nanocrystals, quantum dots

## I. INTRODUCTION

IN recent years, much attention has been devoted to the investigation of the luminescence properties of nano sized silicon (Si) and germanium (Ge) crystals. Various fabrication methods of nanocrystals have been explored intensively to explore the feasibility of integrating Si-based optoelectronic devices.<sup>1-3</sup> In addition to luminescence properties, Si and Ge nanocrystals embedded in silicon oxide matrix has also emerged as a promising candidate for single electron memory devices. A nanocrystal electrically erasable programmable read only memory (EEPROM) cell is essentially a metal-oxide-semiconductor field effect transistor (MOSFET) with nanocrystals acting as electrically isolated charge storage nodules in the oxide. The memory is programmed by applying a gate bias that allows

tunneling of electrons from the silicon substrate through the thin oxide to the nanocrystals. The tunneled electrons get trapped, i.e., stored at the nanocrystals. It has been shown that nanocrystal memory devices have better charge retention, faster write/erase times, higher cyclability and lower power consumption, as compared to conventional nonvolatile memories.<sup>4,5</sup>

Tiwari *et al.* have fabricated memory devices based on Si nanocrystals. Compared to the conventional floating gate devices, the Si nanocrystal based devices exhibited faster write/erase time, lower operating voltage and longer charge retention characteristic.<sup>4</sup> Recently, there have been intensive research on the fabrication of nanocrystalline Ge (nc-Ge) memory devices via the oxidation of silicon germanium ( $\text{Si}_x\text{Ge}_{1-x}$ ) films.<sup>5,8</sup> Despite the considerable effort devoted to this study, there are different explanations for the charge storage mechanism for these devices. The charge has been suggested to be stored at the Ge conduction band<sup>4,6</sup> or at deep traps<sup>7</sup>.

In this study, we synthesized nc-Ge with diameter of ~10 nm via the oxidation of radio frequency (rf) sputtered  $\text{Si}_{0.54}\text{Ge}_{0.46}$  films. We have observed memory effects for the nc-Ge embedded MOS structures fabricated by this technique. The formation of the nc-Ge was investigated using Raman spectroscopy and high resolution transmission electron microscopy (HRTEM). The memory effect of the devices was examined using capacitance versus voltage (C-V) measurements. Fourier transform infrared (FTIR) spectroscopy was employed to monitor the amount of various chemical (Si-O-Si, Si-O-Ge, Ge-O-Ge) bonds in the oxidized  $\text{Si}_{0.54}\text{Ge}_{0.46}$  films to facilitate a discussion on the possible charge storage mechanisms.

## II. EXPERIMENTAL PROCEDURE

We synthesized nc-Ge embedded in a silicon oxide matrix via the wet oxidation of 10 nm-thick  $\text{Si}_{0.54}\text{Ge}_{0.46}$  films. The memory device consisted of a (nc-Ge+ $\text{SiO}_2$ ) layer being sandwiched between a 5 nm-thick tunneling oxide and a cap oxide of 50 nm thickness. The device fabrication sequence is as follows: a tunneling oxide was grown on a

Eric W.H. Kan is a research scholar with Singapore-MIT Alliance, 4 Engineering Drive 3, Singapore 117576 (e-mail: smap1035@nus.edu.sg).

(100)-oriented p-type Si substrate via rapid thermal oxidation at 1000°C for 35 s. A layer of  $\text{Si}_{0.54}\text{Ge}_{0.46}$  film was then deposited by the rf sputtering technique at room temperature in argon (Ar) gas at a pressure of 3.3 mTorr. A typical deposition rate of 4 Å/s was obtained with a rf power of 100 W. The tunnel oxide plus  $\text{Si}_{0.54}\text{Ge}_{0.46}$  film was annealed at 800°C for 6 h in pure nitrogen ( $\text{N}_2$ ) ambient to form a tunnel oxide-polycrystalline  $\text{Si}_{0.54}\text{Ge}_{0.46}$  structure. The thickness and Ge content of the  $\text{Si}_{0.54}\text{Ge}_{0.46}$  film were determined using a step profiler and the Rutherford backscattering technique, respectively. The wet oxidation of  $\text{Si}_{0.54}\text{Ge}_{0.46}$  film was then performed at 600°C for different durations using a conventional three-zone furnace. The structure was then capped with a rf sputtered  $\text{SiO}_2$  gate oxide layer deposited at room temperature to achieve a trilayer (tunnel oxide/oxidized polycrystalline  $\text{Si}_{0.54}\text{Ge}_{0.46}$ /rf sputtered  $\text{SiO}_2$ ) structure. Finally, the trilayer structure was rapid thermal annealed (RTA) in either pure  $\text{N}_2$  or forming gas (90% $\text{N}_2$ +10% $\text{H}_2$ ) ambient using a double step (1000°C for 300 s followed by 700°C for 60 s) annealing process. We have demonstrated earlier that such a double-step annealing process enabled the formation of spherical nc-Ge with good crystallinity, shape and size distribution in the silicon oxide matrix.<sup>9</sup>

The Raman measurements were performed at room temperature with the 514.5 nm line of an Ar laser as the excitation source. The HRTEM experiments were carried out using the Philips FEG 300 CM operating at 300 kV. The C-V measurements were carried out using a Hewlett-Packard LCR analyzer (HP4184A). The FTIR measurements were performed using a Nicolet Magna-IR 850 spectrometer with a resolution of 2  $\text{cm}^{-1}$ .

### III. RESULTS AND DISCUSSION

#### A. Raman and HRTEM studies

Figure 1 shows the Raman spectra for the as-deposited, wet oxidized, and wet oxidized plus RTA trilayer structures. The oxidation was carried out at 600°C for various durations, and the RTA process was performed either in pure  $\text{N}_2$  or forming gas ambient. In Fig. 1, the peaks at  $\sim 300\text{cm}^{-1}$  and  $\sim 400\text{cm}^{-1}$  correspond to the Ge-Ge and Si-Ge vibrations, respectively. For the as-deposited  $\text{Si}_{0.54}\text{Ge}_{0.46}$  film structure, both the Si-Ge and Ge-Ge peaks were present (spectrum (a)). This is reasonable as the  $\text{Si}_{0.54}\text{Ge}_{0.46}$  film is polycrystalline in nature. The Si-Ge peak intensity reduces after oxidation for 15 min (spectrum (b)), and disappears completely after 30 min of oxidation (spectrum (c)). It is interesting to note the presence and sharpening, i.e., the reduction in full width at half maximum (FWHM), of the Ge-Ge peak in case (c). This Ge-Ge peak, however, is nearly absent when the film has been oxidized for 50 min (see spectrum (d)). Thermodynamically, a complete wet oxidation of  $\text{Si}_{0.54}\text{Ge}_{0.46}$  films at 600°C should yield only mixed oxide.<sup>10</sup> We believe a complete oxidation of the  $\text{Si}_{0.54}\text{Ge}_{0.46}$  film was achieved after a duration of 50 min. As for the film that was oxidized for a shorter duration (i.e., 30 min), given the

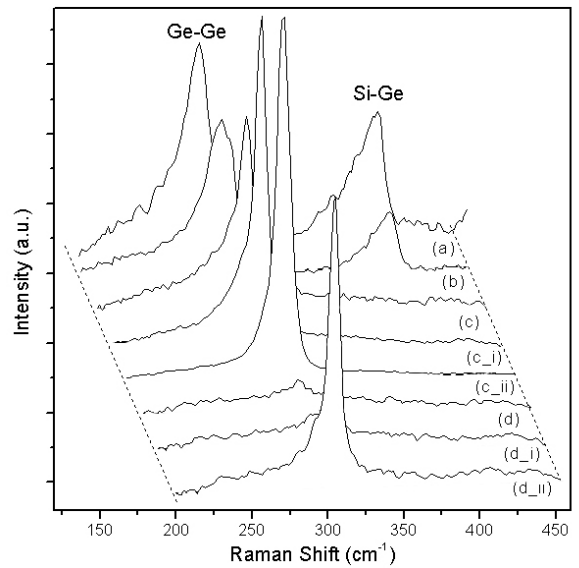


Fig. 1. A series of Raman spectra of (a) as-prepared polycrystalline  $\text{Si}_{0.54}\text{Ge}_{0.46}$  film; (b) polycrystalline  $\text{Si}_{0.54}\text{Ge}_{0.46}$  film oxidized for 15 min; (c) polycrystalline  $\text{Si}_{0.54}\text{Ge}_{0.46}$  film oxidized for 30 min, (c\_i) and (c\_ii) polycrystalline  $\text{Si}_{0.54}\text{Ge}_{0.46}$  film oxidized for 30 min and subsequent annealing in pure  $\text{N}_2$  and forming gas, respectively; (d) polycrystalline  $\text{Si}_{0.54}\text{Ge}_{0.46}$  film oxidized for 50 min, (d\_i) and (d\_ii) polycrystalline  $\text{Si}_{0.54}\text{Ge}_{0.46}$  film oxidized for 50 min and subsequent annealing in pure  $\text{N}_2$  and forming gas, respectively.

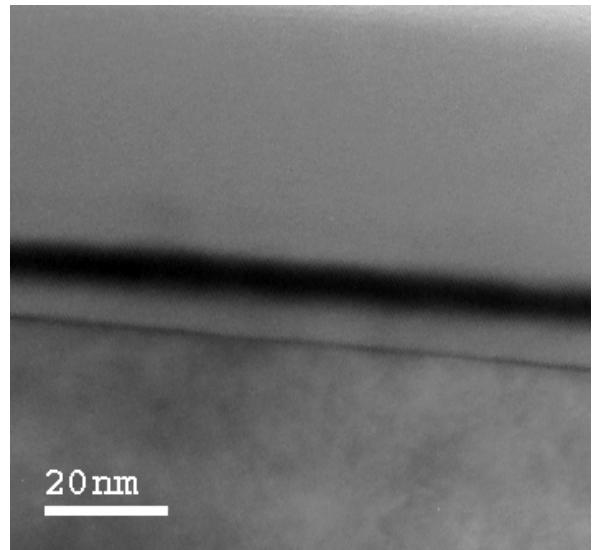


Fig. 2. Cross-sectional TEM image of 10 nm  $\text{Si}_{0.54}\text{Ge}_{0.46}$  film that has been wet oxidized for 30 min at 600°C.

higher binding energy of Si-Ge as compared to Ge-Ge bonds,<sup>11</sup> one should expect the Ge-Ge bond to break before the Si-Ge bond; namely, the Ge-Ge peak should disappear before the Si-Ge peak in a Raman spectrum. However, the Raman spectrum of the film that was oxidized for 30 min (spectrum (c)) shows a reverse trend. We explain this together with the TEM data in the next paragraph.

Figure 2 shows the cross-sectional HRTEM image of the  $\text{Si}_{0.54}\text{Ge}_{0.46}$  film that has been oxidized for 30 min. The dark middle layer, which corresponds to the oxidized  $\text{Si}_{0.54}\text{Ge}_{0.46}$  film, has a similar thickness ( $\sim 10$  nm) to that of the original poly- $\text{Si}_{0.54}\text{Ge}_{0.46}$  layer. The absence of the Si-Ge peak in

spectrum (c) of Fig. 1 suggests that Si atoms in the  $\text{Si}_{0.54}\text{Ge}_{0.46}$  have been fully oxidized. There are no observable lattice fringes from the dark layer indicating that the film is predominantly amorphous. As the oxidized layer is uniform and there is no evidence of Ge pile-up at the  $\text{Si}_{0.54}\text{Ge}_{0.46}$ -tunnel oxide interface, the presence of the Ge-Ge peak in spectrum (c) of Fig. 1 must be due to Ge nanocrystallites distributed evenly in the oxidized film. The formation of the nanocrystallites could be due to the following process. In the oxidation of  $\text{Si}_{0.54}\text{Ge}_{0.46}$  films, the Si and Ge atoms are oxidized to form Si-O and Ge-O bonds. It is possible that some of the Ge-O bonds (either from  $\text{GeO}_2$  or  $\text{GeO}_x$  molecule) are reduced back to Ge atoms by Si atoms from the  $\text{Si}_{0.54}\text{Ge}_{0.46}$  film. The Ge atoms can then form the nanocrystallites in the mixed oxide matrix. When the oxidation duration was increased to 50 min, as all the available Si atoms would have been oxidized, one would then expect the oxidation of the Ge nanocrystallites to take place and hence the disappearance of the Ge-Ge peak in the Raman spectrum of such a sample.

Trilayer structures, with the middle layer oxidized for 30 min were annealed in pure  $\text{N}_2$  or forming gas to synthesize nc-Ge. The Raman spectrum of a sample annealed in  $\text{N}_2$  is denoted as (c\_i) in Fig. 1 and the planar HRTEM image is shown in Fig. 3(a). From the TEM images, the mean diameter ( $\delta$ ) of the nc-Ge was estimated to be  $9.48 \pm 1.61$  nm with an area density of  $\sim 5 \times 10^{11} \text{ cm}^{-2}$ . It can be seen from the inset of Fig. 3(a) that the nc-Ge exhibit good crystallinity. This has also been confirmed previously using TEM electron diffraction patterns.<sup>9</sup> The Raman spectrum of the trilayer structure that had been annealed in forming gas is shown as (c\_ii) in Fig. 1 and the corresponding planar HRTEM is shown in Fig. 3(b). Compared to the nc-Ge synthesized in pure  $\text{N}_2$ , no distinct differences are observed in terms of size ( $\delta \sim 10$  nm), shape, crystallinity (see inset of Fig. 3(b)) and density ( $\sim 5.0 \times 10^{11} \text{ cm}^{-2}$ ) of the nanocrystals.

Note the near absence of the Ge-Ge peak of spectrum (d\_i) in Fig. 1 from the trilayer structure with the  $\text{Si}_{0.54}\text{Ge}_{0.46}$  layer that was oxidized for 50 min and annealed in pure  $\text{N}_2$ . Since the annealing was done at 1 atm, direct decomposition of  $\text{GeO}_x$  by thermal energy is not feasible thermodynamically. Without the presence of  $\text{H}_2$  as a reducing agent, we expect the film would consist of mixed oxide entirely, as shown in spectrum (d\_i). On the other hand, a sharp Ge-Ge peak is observed in spectrum (d\_ii) from the trilayer structure with a  $\text{Si}_{0.54}\text{Ge}_{0.46}$  layer that was oxidized for 50 min and annealed in forming gas. Hence, a relatively low temperature ( $600^\circ\text{C}$ ) wet oxidation process of  $\text{Si}_{0.54}\text{Ge}_{0.46}$  films can either give rise to a system of mixed oxide embedded with elemental Ge (for 30 min oxidation) or of mixed oxide entirely (for 50 min oxidation). While it is possible to synthesize Ge nanocrystals via RTA of the oxide film, either in  $\text{N}_2$  or forming gas ambient, from the trilayer structure with middle layer oxidized for 30 min, nanocrystal formation can only be achieved in forming gas annealing for the trilayer structure with middle layer that has been oxidized for 50 min.

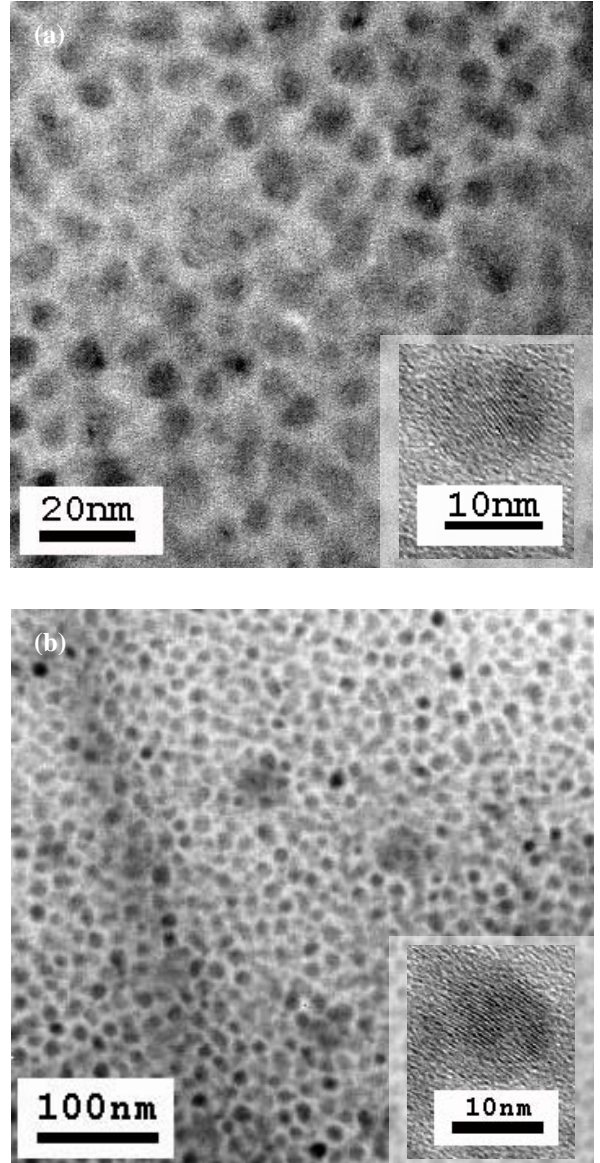


Fig. 3. Planar TEM image of nc-Ge for sample annealed at  $1000^\circ\text{C}$  (300 s) followed by  $700^\circ\text{C}$  (60 s) in (a) pure nitrogen and (b) in forming gas ambient. The insets show enlarged nc-Ge of 10 nm in diameter with clear lattice fringes in both cases.

### B. Capacitance-Voltage measurement

Figure 4 shows typical high-frequency (100 kHz) C-V characteristics of Al-gate capacitors with middle layer that had been oxidized for 30 or 50 min, and subsequently RTA in  $\text{N}_2$  or forming gas ambient (i.e., samples from spectra (c\_i), (c\_ii), (d\_i) and (d\_ii) of Fig. 1). The measurements were performed at room temperature with a constant sweep rate of  $0.25 \text{ Vs}^{-1}$ . All samples were held for 180 s at +10 V before being swept to -10 V and then held at this voltage for 180 s before returning to +10 V. The holding time ensured that the structure was fully charged or discharged at the holding bias before commencement of the C-V sweep and any change in the sweep rate would not affect the flat band voltage shift,  $\Delta V_{\text{FB}}$ , as observed by Kim *et al.*<sup>12,13</sup>

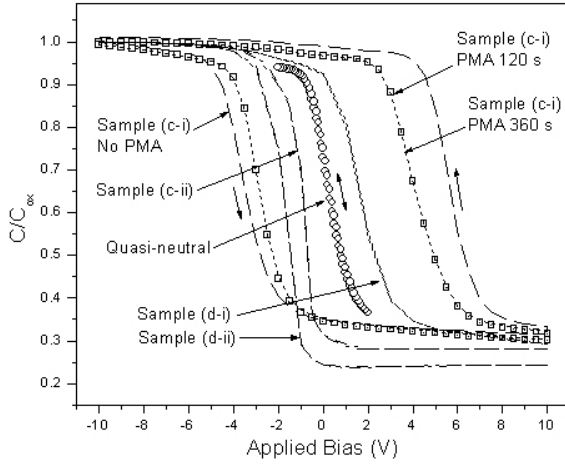


Fig. 4. High frequency C-V curves for trilayer devices with middle layer that had been oxidized for 30 min or 50 min, and subsequently RTA in  $N_2$  or forming gas ambient. Note that post metal annealing (PMA) was performed for all the devices at  $450^\circ\text{C}$  in forming gas ambient.

It is clear that only device (c<sub>i</sub>), with middle layer oxidized for 30 min and subsequently RTA in pure  $N_2$  ambient, shows an anti-clockwise hysteresis with  $\Delta V_{\text{FB}}$  of 9.2 V. A post-metal-annealing (PMA) was performed on this device for 120 s at  $450^\circ\text{C}$  in forming gas ambient. A reduction in the hysteresis was observed indicating possible passivation of trapping sites by the hydrogen species in the forming gas. However, a longer PMA anneal up to 360 s shows no further reduction in hysteresis width. An estimation of the stored charge density was carried out by integrating the area of the hysteresis loop and a charge density of  $1.45 \times 10^{12} \text{ cm}^{-2}$  was obtained. We obtained the quasi-neutral curve by limiting the gate bias sweep range (-2 V to +2 V) and the holding time (1 s) during C-V measurements. This enables the density of the stored negative ( $7.6 \times 10^{11} \text{ cm}^{-2}$ ) and positive ( $6.9 \times 10^{11} \text{ cm}^{-2}$ ) charges to be calculated by estimating the area enclosed between the quasi-neutral C-V and the right-hand or left-hand branch of the C-V characteristic.

As for device (c<sub>ii</sub>), with middle layer oxidized for 30 min and annealed in forming gas ambient, no hysteresis is observed in Fig. 4. The slope at the transition of the C-V curve is also steeper in comparison to that of device (c<sub>i</sub>). Since nc-Ge is present in both trilayer structures (c<sub>i</sub>) and (c<sub>ii</sub>) (see Fig. 3), it is obvious that the charges stored in the system are not located in the conduction band of the nc-Ge. As for devices with middle layer oxidized for 50 min, neither annealing in pure  $N_2$  (d<sub>i</sub>) nor forming gas (d<sub>ii</sub>) ambient exhibits memory effect in the C-V curves. Finally, an appreciably steeper slope in the C-V curve is again observed for samples annealed in forming gas ambient which suggests that the hydrogen species in the forming gas has the effect of both passivating the interface traps at the surface of the nanocrystals (that leads to the disappearance of hysteresis) as well as the traps at the tunnel oxide-Si interface (that leads to a C-V curve with steeper slope). The absence of hysteresis in the device that consists of purely mixed oxide (sample (d<sub>i</sub>)) means that charge storage is not

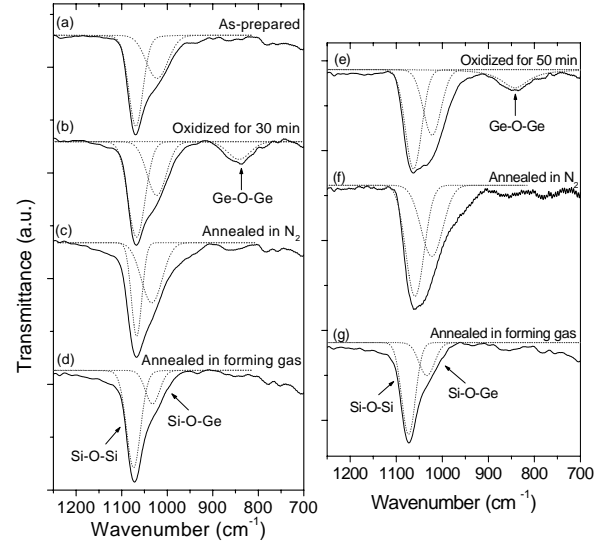


Fig. 5. FTIR spectra of (a) as-prepared  $\text{Si}_{0.54}\text{Ge}_{0.46}$  film, (b)  $\text{Si}_{0.54}\text{Ge}_{0.46}$  film that have been oxidized for 30 min, (c) and (d)  $\text{Si}_{0.54}\text{Ge}_{0.46}$  films that have been oxidized for 30 min and subsequently annealed in  $N_2$  or forming gas, respectively, (e)  $\text{Si}_{0.54}\text{Ge}_{0.46}$  film that have been oxidized for 50 min, (f) and (g)  $\text{Si}_{0.54}\text{Ge}_{0.46}$  films that have been oxidized for 50 min and subsequently annealed in  $N_2$  or forming gas, respectively.

due to the bulk defects in the oxide, i.e., non-bridging oxygen atoms.

### C. FTIR studies

Figure 5 shows the FTIR spectra of the as-deposited, wet oxidized, and wet oxidized plus RTA trilayer structures. In spectrum (a), the peak at  $1000$  to  $1100 \text{ cm}^{-1}$  can be de-convoluted into the stretching mode of Si-O-Si ( $\sim 1075 \text{ cm}^{-1}$ ) and the Si-O-Ge ( $\sim 1030 \text{ cm}^{-1}$ ) bonds. It is also interesting to note from spectra (b) and (e) the existence of Ge-O-Ge ( $\sim 840 \text{ cm}^{-1}$ ) bonds. We have estimated the amount of the Si-O-Ge and Ge-O-Ge bonds from these spectra and found that both types of bonds increased as oxidation duration increased. We have suggested earlier in Section A that the longer oxidation duration of 50 min converts the elemental Ge in the oxide matrix to  $\text{GeO}_x$ . This can account for the increase in the Si-O-Ge and Ge-O-Ge bonds as oxidation duration increased.

Note that when the oxidized films were exposed to RTA in either  $N_2$  or forming gas ambient (see spectra (c), (d), (f) and (g)), there is a drastic reduction in the Ge-O-Ge bonds. There is, however, a pronounced reduction in the Si-O-Ge bonds only for films annealed in forming gas ambient (samples (d) and (g)). We would like to suggest that the Ge-O-Ge bonds may be reduced by  $\text{SiO}_x$  when annealed in  $N_2$ .<sup>9</sup> As for forming gas annealing, the presence of  $\text{H}_2$  reduces Ge-O bonds from both Ge-O-Ge and Si-O-Ge bonds. Note that nanocrystals were observed in the trilayer structures shown in spectra (c), (d) and (g) but only the structure in spectrum (c) exhibited memory effect. We have demonstrated in sections A and B that: (i) annealing the trilayer structure with 30 min oxidized middle layer in  $N_2$  ambient causes the nanocrystallites to combine and form nc-Ge, which exhibits hysteresis in the C-V characteristic, (ii) annealing in  $N_2$  for the trilayer structure with middle

layer oxidized for 50 min does not result in nc-Ge formation and no memory effect, and (iii) forming gas anneal of the trilayer structures with both 30 or 50 min oxidized middle layer results in nc-Ge embedded in the oxide matrix but no memory effect. This clearly indicates that the charge storage mechanism in our devices is closely related to the reduction of Si-O-Ge bonds by the hydrogen in forming gas. We will further discuss this in Section D.

#### D. Charge trapping mechanism

We have suggested that it is unlikely that charges were stored at the conduction band of nc-Ge or bulk oxide defects. The charge storage mechanism is closely related to the reduction of Si-O-Ge bonds by H atoms. The Si-O-Ge bonds are most likely to be located at the outer surface of the nc-Ge where the Ge atoms form bonds with the SiO<sub>x</sub> matrix. It has been reported that a very high interface trap density of the order of 10<sup>12</sup> eV<sup>-1</sup> cm<sup>-2</sup> was obtained from oxidized Si<sub>x</sub>Ge<sub>1-x</sub> films with Ge atoms segregated to the oxide interface.<sup>14,15</sup> It may be reasonable to expect the disappearance of the hysteresis in the C-V curves of devices annealed in forming gas as the hydrogen atoms may passivate the trapping sites. Note that for H<sub>2</sub> introduced at a lower temperature during PMA (450°C) for 360 s (i.e., same as the RTA duration), the hysteresis remained fairly constant.

It is possible that during RTA at 1000°C in forming gas ambient, H atoms can reduce GeO<sub>x</sub> (i.e., Si-O-Ge bonds) and subsequently passivate the Ge dangling bonds at the interface of the nc-Ge. At a lower temperature annealing step, such as during PMA, H atoms are prevented from passivating the trapping sites by the thin layer of mixed oxide (i.e., Si-O-Ge) enfolding the core nc-Ge. H<sub>2</sub> may reduce the GeO<sub>x</sub> in the thin layer of mixed oxide but the reaction rate is expected to be extremely slow due to low thermal energy.

#### IV. CONCLUSION

Wet thermal oxidations of polycrystalline Si<sub>0.54</sub>Ge<sub>0.46</sub> films at 600°C for different durations were carried out. It was found that for films oxidized for 50 min, a stable mixed oxide was formed. For films oxidized for 30 min, however, a mixed oxide with Ge nanocrystallites embedded in the oxide matrix was obtained. In capacitors with trilayer gate dielectric stacks consisting of tunnel oxide/oxidized polycrystalline Si<sub>0.54</sub>Ge<sub>0.46</sub>/rf sputtered SiO<sub>2</sub> layers, it was observed that annealing in N<sub>2</sub> ambient, when the middle layer had been oxidized for 30 min, causes the nanocrystallites to combine and form nc-Ge that exhibits memory effect. However, annealing in N<sub>2</sub>, when the middle layer had been oxidized for 50 min, did not result in nc-Ge formation and no memory effect. Finally, it was observed that annealing the trilayer structures with either 30 or 50 min oxidized middle layer in forming gas ambient results in nc-Ge embedded in the oxide matrix but with no memory effect. We have proposed that the charge storage mechanism for the trilayer structure is closely related to interface traps

of the nc-Ge.

#### ACKNOWLEDGMENT

The authors would like to thank the Singapore-MIT Alliance and the National University of Singapore for supporting this work.

#### REFERENCES

- [1] Shinji Takeoka, Minoru Fujii and Shinji Hayashi, Phys. Rev. B **62**, 16 820 (2000).
- [2] Shinji Takeoka, Kimiaki Toshikiyo, Minoru Fujii, Shinji Hayashi and Keiichi Yamamoto, Phys. Rev. B **61**, 15 988 (2000).
- [3] Shinji Takeoka, Minoru Fujii, Shinji Hayashi and Keiichi Yamamoto, Phys. Rev. B **58**, 7921 (1998).
- [4] S. Tiwari, F. Rana, H. Hanafi, A. Hartstein, E. F. Crabbé and K. Chan, Appl. Phys. Lett. **68**, 1377 (1966).
- [5] Y.-C. King, T.-J. King and C. Hu, IEEE Trans. Electron Devices **48**, 696 (2001).
- [6] T. Kobayashi, T. Endoh, H. Fukuda, S. Nomura, A. Sakai and Y. Ueda, Appl. Phys. Lett. **71**, 1195 (1997).
- [7] Y. Shi, K. Saito, H. Ishikuro and T. Hiramoto, Appl. Phys. Lett. **84**, 2358 (1998).
- [8] E.W.H. Kan, C.C. Leoy, W.K. Choi, W.K. Chim, D.A Antoniadis and E.A. Fitzgerald (Unpublished data)
- [9] E.W.H. Kan, W.K. Choi, C.C. Leoy, W.K. Chim, D.A Antoniadis and E.A. Fitzgerald, Appl. Phys. Lett. **83**, 2058 (2003).
- [10] S.-G. Park, W.S. Liu and M.-A. Nicolet, J. Appl. Phys. **75**, 1746 (1994).
- [11] R. W. Olenski and G. J. Abbaschian, Bull. Alloy Phase Diagrams, **5**(2), 1984 (Based on the higher melting temperature of silicon germanium alloy as compared to elemental germanium).
- [12] Yong Kim, Kyung Hwa Park, Tae Hun Chung, Hong Jun Bark, Jae-Yel Yi, Won Chel Choi, Eun Kyu Kim, Ju Wook Lee and Jeong Yong Lee, Appl. Phys. Lett. **78**, 934 (2001).
- [13] Yong Kim, Hea Jong Cheong, Kyung Hwa Park, Tae Hun Chung, Hong Jun Bark, Jae-Yel Yi, S H Bang and J H Cho, Semicond. Sci. Technol. **17**, 1039 (2002).
- [14] F.K. LeGoues, R. Rosenberg, T. Nguyen, F. Himpsel and B.S. Meyerson, J. Appl. Phys. **65**, 1724 (1989).
- [15] W.K. Choi, A. Natarajan, L.K. Bera, A.T.S. Wee and Y.J. Liu, J. Appl. Phys. **91**, 2443 (2002).